

MAGNETIC STRUCTURES IN GAMMA-RAY BURST JETS PROBED BY GAMMA-RAY POLARIZATION

DAISUKE YONETOKU¹, TOSHIO MURAKAMI¹, SHUICHI GUNJI², TATEHIRO MIHARA³, KENJI TOMA⁴, YOSHIYUKI MORIHARA¹, TAKUYA TAKAHASHI¹, YUDAI WAKASHIMA¹, HAJIME YONEMOCHI¹, TOMONORI SAKASHITA¹, NORIYUKI TOUKAIRIN², HIROFUMI FUJIMOTO¹, AND YOSHIKI KODAMA¹,

Not to appear in Nonlearned J., 45.

ABSTRACT

We report polarization measurements in two prompt emissions of gamma-ray bursts, GRB 110301A and GRB 110721A, observed with the Gamma-ray burst polarimeter (GAP) aboard IKAROS solar sail mission. We detected linear polarization signals from each burst with polarization degree of $\Pi = 70 \pm 22$ % with statistical significance of 3.7σ for GRB 110301A, and $\Pi = 84^{+16}_{-28}$ % with 3.3σ confidence level for GRB 110721A. We did not detect any significant change of polarization angle. These two events had shorter durations and dimmer brightness compared with GRB 100826A, which showed a significant change of polarization angle, as reported in Yonetoku et al. (2011b). Synchrotron emission model can be consistent with all the data of the three GRBs, while photospheric quasi-thermal emission model is not favorable. We suggest that magnetic field structures in the emission region are globally-ordered fields advected from the central engine.

Subject headings: gamma-ray burst: individual (GRB 110301A, GRB 110721A) – instrumentation: polarimeters – polarization – radiation mechanisms: non-thermal – relativistic processes

1. INTRODUCTION

Gamma-ray bursts (GRBs) are the most energetic explosions in the universe. Since the discovery of GRBs in late 1960s, spacial distribution (directions and redshifts), lightcurves and energy spectra have been observed for large amount of GRBs. However, the emission mechanism of prompt GRBs, how to release the huge energy in short time duration, is still a crucial issue. The other characteristic of electro-magnetic wave, i.e. polarization in gamma-ray band, is thought to be a key to solve the problem. Polarization measurement can probe the existence of magnetic fields, and/or some kinds of geometrical structures, which are difficult to be examined from time variability and energy spectra.

Several previous works reported marginal detections of linear polarization. Coburn & Boggs (2003) reported the detection of strong polarization from GRB 021206 by *RHESSI*. However, independent authors analyzed the same *RHESSI* data, and concluded that any polarization signals were not confirmed (Rutledge & Fox 2004; Wigger et al. 2004). Kalemci et al. (2007); McGlynn et al. (2007); Götz et al. (2009) reported marginal detections of polarization with $\sim 2\sigma$ confidence from GRB 041219 by *INTEGRAL*-SPI and -IBIS data. As the authors themselves discussed that the possibility of instrumental systematics could not be completely removed, and a part of these results were obviously inconsistent with each other (see Section 1 of Yonetoku et al. 2011b). Therefore, further observations with reliable instruments are strongly required to confirm the existence of polarization in prompt GRBs.

Recently, Gamma-ray burst polarimeter (GAP;

Yonetoku et al. 2006, 2011a; Murakami et al. 2010) aboard the *IKAROS* solar-power-sail (Kawaguchi et al. 2008; Mori et al. 2009) measured a linear polarization of $\Pi = 27 \pm 11$ % with 2.9σ confidence level in extremely bright GRB 100826A (Yonetoku et al. 2011b). It was found that the polarization angle changes during the prompt emission with 3.5σ confidence level. The GAP detector is designed for the gamma-ray polarimetry of prompt GRBs, and also realized the quite small systematic uncertainty of 1.8 % level (Yonetoku et al. 2011a). This may be the most convincing detection of polarization degree so far. But this is only one case, we need more sample to establish the existence of gamma-ray polarization in prompt GRBs. In this Letter, we report two more detections of gamma-ray polarization in GRB 110301A and GRB 110721A observed with *IKAROS*-GAP. We analyzed all data observed by GAP until the end of 2011, and found significant polarization signals from these events.

2. OBSERVATIONS

We observed two GRBs, GRB 110301A and GRB 110721A, with the Gamma-Ray Burst Polarimeter (GAP) aboard the *IKAROS* solar power sail. The polarization detection principle of GAP is to measure the anisotropic distribution against the Compton scattering angle. According to the Klein-Nishina cross section, the gamma-ray photons tend to scatter toward the vertical direction of polarization vector. Therefore the modulation against the azimuth scattering angle is observed if the incident gamma-rays are polarized. The advantages of GAP are the high axial symmetry in shape and the high gain uniformity. These are the key to reduce the instrumental systematic uncertainties. Details of the GAP detector are shown in Yonetoku et al. (2011a).

The GAP detected GRB 110301A on 2011 March 1 at 05:05:34.9 (UT) at 0.946 AU away from the Earth. This burst was also detected by *Fermi*-GBM. The coordinate was determined as $(\alpha, \delta) = (229.35, +29.40)$ with an uncertainty of 1.0 degrees in radius (Foley et al. 2011), which corresponds to 48 ± 1 deg off-axis from the center of GAP field of view. Figure 1 (top) shows the lightcurve of GRB 110301A observed

yonetoku@astro.s.kanazawa-u.ac.jp

¹ College of Science and Engineering, School of Mathematics and Physics, Kanazawa University, Kakuma, Kanazawa, Ishikawa 920-1192, Japan

² Department of Physics, Faculty of Science, Yamagata University, 1-4-12, Koshirakawa, Yamagata, Yamagata 990-8560, Japan

³ Cosmic Radiation Laboratory, RIKEN, 2-1, Hirosawa, Wako City, Saitama 351-0198, Japan

⁴ Department of Earth and Space Science, Osaka University, Toyonaka 560-0043, Japan

with GAP in the energy range of 70–300 keV.

According to the time resolved spectral analyses by Lu et al. (2012), the spectral peak energy (E_p) slightly changes during the burst, and show hard to soft trend from 110 keV to 26 keV. Therefore GAP mainly observed the energy range of $E > E_p$. The energy fluence in 10–1,000 keV is $(3.65 \pm 0.03) \times 10^{-5}$ erg cm $^{-2}$ (Foley et al. 2011).

GRB 110721A was detected on 2011 July 21 at 04:47:38.9 (UT) at 0.699 AU from the Earth. Figure 1 (bottom) shows the lightcurve of GRB 110721A. This burst was first discovered by *Fermi*-GBM and LAT (Tierney et al. 2011; Vasileiou et al. 2011). After that, the *Swift*-XRT performed the follow-up observation of its X-ray afterglow (Greiner et al. 2011; Grupe et al. 2011). The coordinate is precisely measured as $(\alpha, \delta) = (333.66, -38.59)$ which corresponds to 30 deg off-axis. The optical transient was also detected by GROND (Greiner et al. 2011) and its redshift was measured as $z = 0.382$ from two absorption lines of CaII with Gemini-South (Berger et al. 2011).

The spectral parameters, especially the E_p values, dramatically change during the burst (Tierney et al. 2011; Golenetskii et al. 2011; Lu et al. 2012). The E_p around the maximum intensity is about $E_p = 1130^{+550}_{-490}$ keV, and the one of time integrated spectrum is $E_p = 393^{+199}_{-104}$ keV. GAP mainly observed in the energy range of $E < E_p$. The energy fluence in 10–1,000 keV is $(3.52 \pm 0.03) \times 10^{-5}$ erg cm $^{-2}$ (Tierney et al. 2011), which is very similar to GRB 110301A.

3. DATA ANALYSES

3.1. Average Properties of Polarization

We analyzed polarization data during the time intervals between two dashed lines shown in Figure 1 for GRB 110301A and GRB 110721A, respectively. GAP obtained the polarization data between -16 s to 176 s since the GRB trigger. Since the time durations of these GRBs are relatively short, we used the background obtained in the same data. The net background rate for the polarization data is 60.0 counts s $^{-1}$ for GRB 110301A and 51.6 counts s $^{-1}$ for GRB 110721A. The total numbers of gamma-ray photons after subtracting the background are 1,820 and 1,092 photons for each burst, respectively.

To estimate the systematic uncertainty, we first consider the spin rate of *IKAROS* spacecraft. The rotation of instrument generally reduces the systematic uncertainty because the differences of each sensor and the geometrical skewness are averaged. However, in these case, the time durations of bursts are smaller than the period of rotation of *IKAROS* spacecraft. The spin rate is 1.61 rpm and 0.22 rpm for the epoch of GRB 110301A and GRB 110721A, respectively. Using the background interval of the data, we created the history of background modulation curves with the same time interval we analyzed, and confirmed each modulation was consistent with constant within the statistical error. We confirmed the systematic error due to the data analysis of short time duration is about $\sigma_{\text{sys},1} = 1.0$ % of the total polarization signals for each bin of both GRBs.

Next, we estimated the systematic uncertainty between the detector response calculated by the Geant 4 simulator and the experimental data, which is mainly due to the off-axis direction of incident gamma-rays. We performed several ground experiments described in Yonetoku et al. (2011b) with the proto-flight model of GAP. We estimated the systematic uncertainty was $\sigma_{\text{sys},2} = 1.9$ % of the total polarization signals

for each bin.

In Figure 2, we show the modulation curve (polarization signals) after subtraction of the background. The error bars accompanying with the data (filled circles) includes not only the statistical error (σ_{stat}) but also the systematic uncertainties described above. The total errors are calculated as $\sigma_{\text{total}}^2 = \sigma_{\text{stat}}^2 + \sigma_{\text{sys},1}^2 + \sigma_{\text{sys},2}^2$ for each bin of polarization data.

The model functions (detector responses) were calculated with the Geant 4 simulator considering the spectral evolutions reported by Lu et al. (2012), who performed spectral analyses for 20 and 14 time intervals of GRB 110301A and GRB 110721A, respectively. Using their spectral parameters, we simulated the model functions for each time interval, and also combined into the one with the appropriate weighting factor estimated with the brightness histories.

In these analyses, the free parameters are the polarization degrees (Π) and angles (ϕ_p). We simulated the model function with step resolutions of 5 % for polarization degree and 5 deg for phase angles. In Figure 2, we show the best fit model with solid black lines, and also superposed the non-polarization model as the dashed lines on the same panel for easy comparison. The best fit parameters are $\Pi = 70 \pm 22$ % and $\phi_p = 73 \pm 11$ deg with $\chi^2 = 14.0$ for 10 degree of freedom (d.o.f) for GRB 110301A, and $\Pi = 84^{+16}_{-28}$ % and $\phi_p = 160 \pm 11$ deg with $\chi^2 = 7.3$ for 10 d.o.f for GRB 110721A, respectively. Here the quoted error are at 1 σ confidence for two parameters of interest (Π and ϕ_p), and the ϕ_p is measured counterclockwise from the celestial north.

We show $\Delta\chi^2$ maps in the (Π, ϕ_p) plane in Figure 3. The white dots are the best fit results, and we calculate $\Delta\chi^2$ values relative to these points. The 1 σ , 2 σ and 3 σ confidence contours for two parameters of interest are shown in the same figures. The null hypothesis (zero polarization degree) can be ruled out with 3.7 σ (99.98 %) for GRB 110301A, and 3.3 σ (99.91 %) confidence levels, respectively. Although these results have relatively large errors compared with the previous GAP result for GRB 100826A ($\Pi = 27 \pm 11$ %, 2.9 σ significance level), the polarization degree of these two GRBs may be larger than that of GRB 100826A. From these observations, we conclude the gamma-ray polarization really exists in the prompt GRBs.

3.2. Time Resolved Polarization Analyses

Yonetoku et al. (2011b) found a significant change of polarization angle in very bright GRB 100826A. Therefore we also tried to investigate the existence of such effect in these two GRBs.

As shown in Figure 1 (top), two main peaks exist in the lightcurve of GRB 110301A. We divided the polarization data into two parts in time, i.e. $0 \text{ s} \leq t < 3 \text{ s}$ and $3 \text{ s} \leq t < 7 \text{ s}$. Here t is the time since trigger. The fitting results are $\Pi = 65 \pm 28$ % and $\phi_p = 73 \pm 14$ deg for the first half part, and $\Pi = 80^{+20}_{-39}$ % and $\phi_p = 71 \pm 15$ deg for the second half part. The significance of polarization detection is 2.87 σ and 2.56 σ , respectively.

The brightest part of GRB 110721A lightcurve shows rather flatter compared with the standard “fast-rise and exponential decay” of GRBs, and we divided the polarization data into $0 \text{ s} \leq t < 2 \text{ s}$ and $2 \text{ s} \leq t < 11 \text{ s}$. The best fit results are $\Pi = 81^{+19}_{-40}$ % and $\phi_p = 155 \pm 14$ deg for the first part and $\Pi = 78^{+22}_{-43}$ % and $\phi_p = 164 \pm 17$ deg for the second part. The significance is 2.55 σ and 2.16 σ , respectively.

We analyzed the polarization data of several time inter-

vals, but we could not find any significant change of polarization angle and degree. In these two cases, we conclude the polarization angles are stable during the prompt emission within the error. This is quite different properties from GRB 100826A by Yonetoku et al. (2011b), and we should consider an explainable conditions of emission mechanism including both polarization properties.

4. DISCUSSION

Major results of the GAP observations so far are simply summarized as follows: (1) there are cases with and without a significant change of polarization angle (PA), and (2) GRB 100826A, with a long duration $T \sim 100$ s, has a PA change, and its polarization degree (PD) is $\Pi = 27 \pm 11\%$, while GRB 110301A and GRB 110721A, with short durations $T \sim 10$ s, have no PA change, and their PDs are $\Pi \gtrsim 30\%$ at 2σ error region (see Figure 3). Here we present some theoretical implications from these observational results for synchrotron and photospheric emission models, following Yonetoku et al. (2011b).

First we discuss synchrotron models with different types of magnetic field structure. One type is helical magnetic fields, which may be advected from the central engine through the jet. Such globally-ordered fields can produce high-PD emission (Granot 2003; Lyutikov et al. 2003). We call this ‘SO model’. In this model, the existence of a significant PA change implies that emission region consists of multiple patches with characteristic angular size θ_p much smaller than the opening angle of the jet θ_j (Yonetoku et al. 2011b). Relativistic beaming effect only allows us to observe angular size of $\sim \Gamma^{-1}$ around the line of sight (LOS), where Γ is the bulk Lorentz factor of the jet. In the case of $\Gamma^{-1} \sim \theta_j$, it is natural that we see multiple patches with different magnetic field directions, and then we observe significant PA changes. On the other hand, if $\Gamma^{-1} \ll \theta_j$, we only see a limited range of the curved magnetic fields, which leads to no significant PA change even for patchy emission. The net PD of the latter case can be estimated as $\Pi \sim 40\%$ for photon index $\Gamma_B \sim -1$ (whereas synchrotron emission from a point source has $\Pi_{\max}^{\text{syn}} = (-\Gamma_B)/(-\Gamma_B + \frac{2}{3})$) (see the case of $y_j = 100$ in Figure 2 of Toma et al. 2009), which is compatible to the observed PD of $\Pi \gtrsim 30\%$ from GRB 110301A and GRB 110721A. Therefore, the case of $\Gamma^{-1} \sim \theta_j$ could correspond to GRB 100826A, while the case of $\Gamma^{-1} \ll \theta_j$ to the other two bursts with no PA change.

We may consider an alternative model in which GRB jets consist of multiple impulsive shells which have globally-ordered transverse magnetic fields with different direction for each shell. Let us call this ‘non-steady SO model’. It has been recently claimed that such impulsive shells can be accelerated to relativistic speeds (Granot et al. 2012). This polarization model may also apply to a scenario in which initial globally-ordered helical fields get distorted, making different field directions within the angular size of Γ^{-1} , as considered in ICMART model (Zhang & Yan 2011). In this model, PA changes can naturally occur, although it does not necessarily occur when the number of shells is small so that T is relatively small. The net PD will be $\Pi \sim \Pi_{\max}^{\text{syn}}/\sqrt{N}$, where N is the number of shells with different field directions. This could be as high as $\Pi_{\max}^{\text{syn}} \sim 60\%$ for $\Gamma_B \sim -1$ when T is relatively small, which is consistent with the observed PD of $\Pi \gtrsim 30\%$.

Shocks formed in the jet may produce sizable magnetic fields with random directions on plasma skin depth scales.

Synchrotron emission from such fields can have high PD, provided that the field directions are not isotropically random but random mainly in the plane parallel to the shock plane (i.e., perpendicular to the local direction of expansion) (Granot 2003; Nakar et al. 2003). We call this ‘SR model’. The linear polarization directions in the observer frame are symmetric around the LOS. Thus, if the emission is patchy, net PD can be nonzero and can have PA changes (Yonetoku et al. 2011b) (see also Lazzati & Begelman 2009). The characteristic angular size of the patches may be hydrodynamically constrained to be $\theta_p \gtrsim \Gamma^{-1}$. In this model, the PD of emission from one patch strongly depends on the viewing angle of the patch θ_v , i.e., the angle between the axis of the patch and the LOS, and it is limited as $\Pi \lesssim 40\%$ (see the cases of $y_j \geq 1$ in Figure 3 of Toma et al. 2009). This implies that fine tuning, $\theta_v \sim \theta_p + \Gamma^{-1}$, is required to have $\Pi > 30\%$. Furthermore, the bursts we observed are all very bright, which suggests that some patches are seen with $\theta_v \lesssim \theta_p$, for which $\Pi \ll 40\%$. This suggests that the SR model is not favorable to explain the observed PD of $\Pi \gtrsim 30\%$.

Internal shocks may also produce strong magnetic fields with random directions on hydrodynamic scales (Inoue et al. 2011; Gruzinov & Waxman 1999). We call this ‘SH model’, which produces net PD as $\Pi \sim \Pi_{\max}^{\text{syn}}/\sqrt{N}$, where N is the number of independent patches with coherent magnetic field in the observable angular size $\sim \Gamma^{-1}$, and can naturally lead to PA changes. Unlike the SR models, the emission from patches seen with small θ_v has high PD, so that this model is in agreement with the high brightness of the bursts. However, recent MHD simulations of internal shocks with initial density fluctuations imply $N \sim 10^3$ (Inoue et al. 2011), which cannot explain the observed PD of $\Pi \gtrsim 30\%$.

Lastly, we discuss photospheric emission (Ph) model. This model assumes that the emission at $E \gtrsim E_p$ is the quasi-thermal radiation from the photosphere. The emission at $E < E_p$ might be a superposition of many of the quasi-thermal components with different temperatures (Ryde et al. 2010; Toma et al. 2011) or contribution from synchrotron emission (Vurm et al. 2011). The quasi-thermal radiation can have high PD when the radiation energy is smaller than the baryon kinetic energy at the photosphere (Beloborodov 2011). The linear polarization directions in the observer frame are symmetric around the LOS, same as the SR model. The PD of emission from a given point may be determined by the brightest emission, coming from just below the photosphere, which can have $\Pi \leq \Pi_{\max}^{\text{qt}} \sim 40\%$ (Beloborodov 2011). The PD of emission from one patch, whose angular size is hydrodynamically constrained to be $\theta_p \gtrsim \Gamma^{-1}$, will reduce to $\Pi \lesssim 30\%$ (in the same way as in the SR model). The patches with small viewing angle θ_v have $\Pi \ll 30\%$. Therefore, the Ph model requires very fine tuning of θ_v to reproduce the PD of GRB 110301A, mainly at $E > E_p$ (i.e., dominated by the quasi-thermal component).

To summarize, (1) the SR, SH and Ph models are not favorable to reproduce all of our polarimetric observation results of the three GRBs, and (2) the SO and non-steady SO could explain all of them.

Recently, early optical polarization from the forward shock of a GRB afterglow has been detected as $\Pi \simeq 10.4 \pm 2.5\%$ (at $t = 149 - 706$ s) for GRB 091208B (Uehara et al. 2012). If the magnetic field directions in the emission region are random on plasma skin depth scales (i.e., the SR model for a shock produced in the circumburst medium), the observed po-

larization reaches a maximum value around the jet break time (~ 1 day) (Lazzati 2006). The measurement of the early polarization, higher than the typical observed late-time polarization of $\sim 1-3\%$ (at $t \sim 1$ day; Covino et al. 2004), thus disfavors this model. This result is consistent with our argument against the SR model for a shock produced within the jet.

The *Fermi* satellite team has suggested that GRB 110721A has a blackbody component with temperature ranging in the $\sim 10-100$ keV (Axelsson et al. 2012), which almost coincide with the GAP range 70–300 keV. However, their fitting model of the integrated spectrum (their Figure 2) includes the blackbody flux as only $\sim 1/5$ th of the total flux in the GAP range. Thus reduction of PD by addition of the blackbody component is small. The polarization degree and angle in the GAP range is practically determined by those of the non-thermal

component, which could be synchrotron emission.

The SO models assume globally-ordered fields in the emission region. On the other hand, observations have suggested that prompt emission has very high efficiency (even $> 90\%$ for some bursts; Zhang et al. 2007; Ioka et al. 2006), which means that energy dissipation, usually involving field distortion, occur globally. Reconciling high PD with high efficiency looks a dilemma, which will have to be resolved in more quantitative modeling.

We thank the referee for several useful comments. This work is supported by the Grant-in-Aid for Young Scientists (S) No.20674002 (DY), Young Scientists (A) No.18684007 (DY), JSPS Research Fellowships for Young Scientists No.231446 (KT), and also supported by the Steering Committee for Space Science at ISAS/JAXA of Japan.

REFERENCES

- Axelsson, M., et al. 2012, submitted (arXiv:1207.6109)
 Berger, E. et al., 2011, GCN Circular, 12193
 Beloborodov, A. 2011, ApJ, 737, 68
 Coburn, W. & Boggs, S. E., 2003, Nature, 423, 415-417
 Covino, S. et al., 2004, ASP, 312, 169
 Foley, S. et al., 2011, GCN Circular, 11771
 Golenetskii, S. et al., 2011, GCN Circular, 12191
 Götz, D. et al., 2009, Astrophys. J. 695, L208-L212
 Granot, J. 2003, ApJ, 596, L17
 Granot, J., Komissarov, S. S., & Spitkovsky, A. 2012, MNRAS, 411, 1323
 Greiner, J. et al., 2011, GCN Circular, 12192
 Grupe, D. et al., 2011, GCN Circular, 12212
 Gruzinov, A., & Waxman, E. 1999, ApJ, 511, 852
 Inoue, T., Asano, K., & Ioka, K. 2011, ApJ, 734, 77
 Ioka, K., Toma, K., Yamazaki, R., & Nakamura, T. 2006, A&A, 458, 7
 Kalemci, E. et al., 2007, Astrophys. J. Supplement, 169, 75-82
 Kawaguchi, J. et al., 2008, Proceedings of the 59th International Astronautical Congress, IAC-08-A3.6.15
 Lazzati, D. et al., 2006, New Journal of Physics, 8, 131
 Lazzati, D., & Begelman, M. C., 2009, ApJ, 700, L141
 Lyutikov, M., Pariev, V. I., & Blandford, R. 2003, ApJ, 597, 998
 Lu, R.-J. et al., 2012, ApJ in press (arXiv:1204.0714)
 McGlynn, S. et al., 2007, A&A, 466, 895-904
 Mori, O. et al., Proceedings of the 2nd International Symposium on Solar Sailing (2009)
 Murakami, T. et al., Proceedings of Deciphering the ancient universe with gamma-ray burst, AIP Conference Proceedings, 1279, 227-230 (2010)
 Nakar, E., Piran T., & Waxman, E. 2003, JCAP, 10, 5
 Rutledge, R. E. & Fox, D. B., 2004, MNRAS, 350, 1288-1300
 Ryde, F., et al. 2010, ApJ, 709, L172
 Tierney, D., von Kienlin, A. et al., 2011, GCN Circular, 12187
 Toma, K., Sakamoto, T., Zhang, B., et al. 2009, ApJ, 698, 1042
 Toma, K., Wu, X.-F., & Mészáros, P. 2011, MNRAS, 415, 1663
 Uehara, T., Toma, K., Kawabata, K. S. 2012, ApJ, 752, L6
 Vasileiou, V. et al., 2011, GCN Circular, 12188
 Vurm, I., Beloborodov, A. M., & Poutanen, J. 2011, ApJ, 738, 77
 Wigger, C. et al., 2004, ApJ, 613, 1088-1100
 Yonetoku, D. et al., 2004, ApJ, 609, 935
 Yonetoku, D. et al., 2006, SPIE, 6266, 62662C-1 - 62662C-9
 Yonetoku, D. et al., 2011a, PASJ, 63, 3
 Yonetoku, D. et al., 2011b, ApJ, 743, L30
 Zhang, B., et al. 2007, ApJ, 655, 989
 Zhang, B., & Yan, H. 2011, ApJ, 726, 90

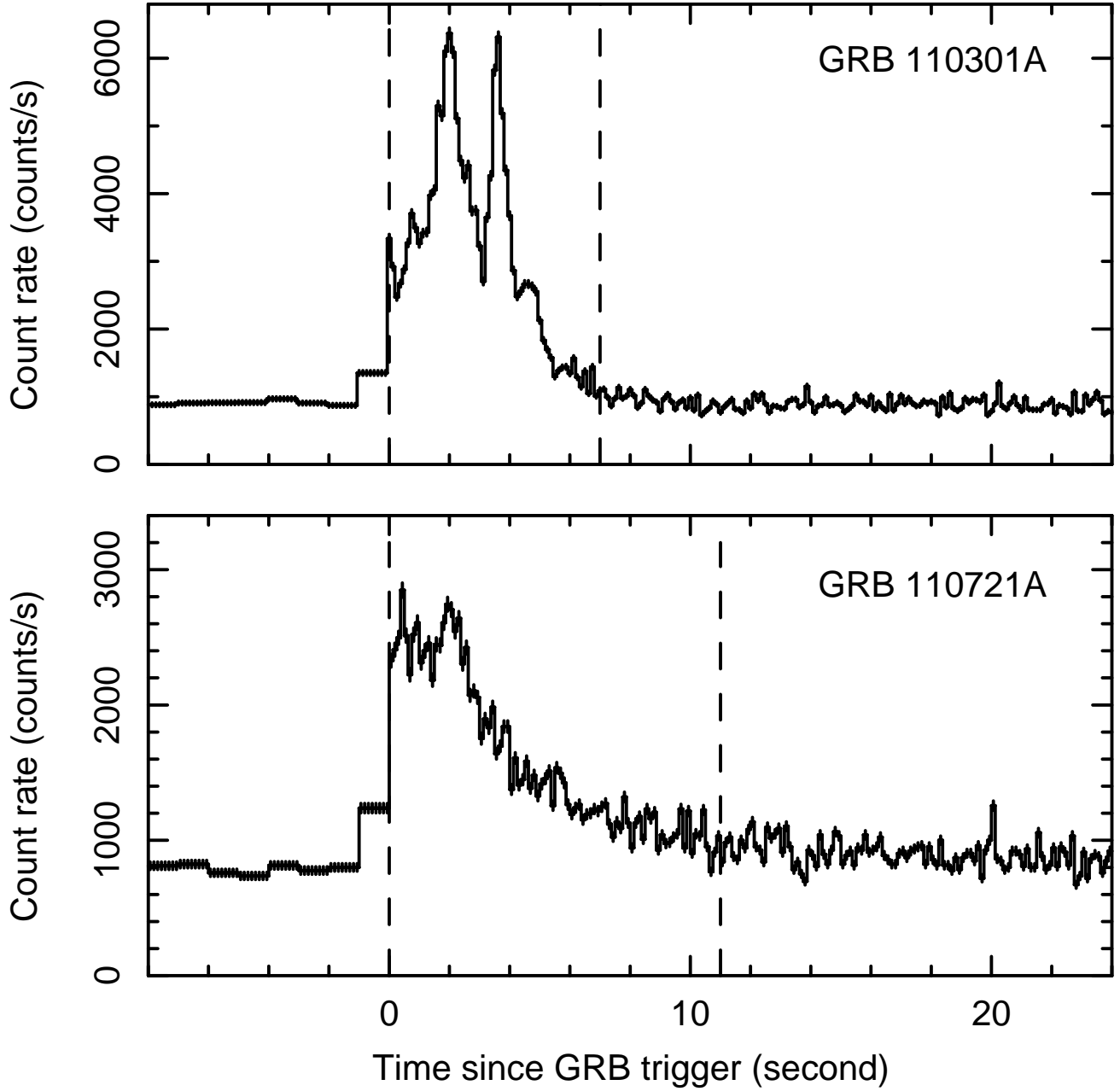


FIG. 1.— Lightcurves of the prompt gamma-ray emission of GRB 110301A (top) and GRB 110721A (bottom) detected by GAP. The vertical dashed lines indicate the time interval of polarization analyses for each burst.

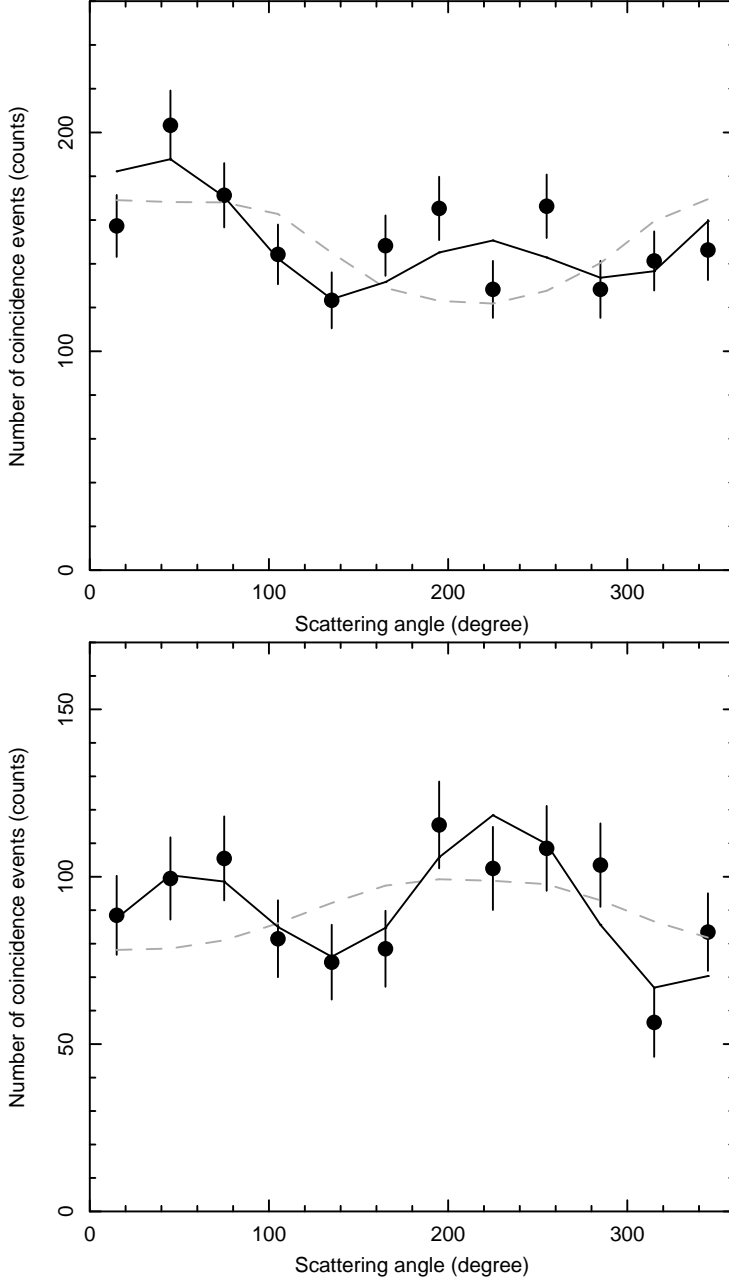


FIG. 2.— Number of coincidence gamma-ray photons (polarization signals) against the scattering angle of GRB 110301A (top) and GRB 110721A (bottom) measured by the GAP in 70–300 keV band. Black filled circles are the angular distributions of Compton scattered gamma-rays after the background subtraction. The solid lines are the best fit models of each event calculated with the Geant4 Monte-Carlo simulations. The model functions of non-polarized cases are superposed on each panel for easy comparison.

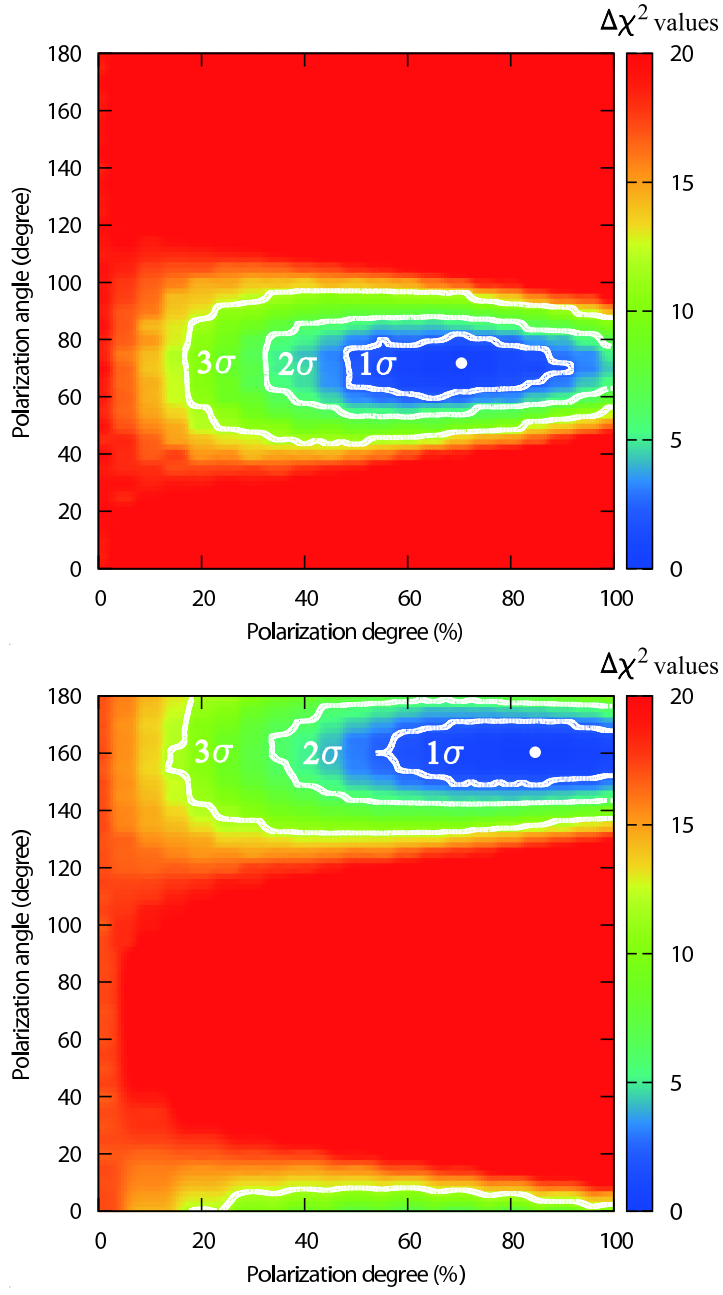


FIG. 3.— Two $\Delta\chi^2$ maps of confidence contours in the (Π, ϕ_p) plane for GRB 110301A (top) and GRB 110721A (bottom). The white dots are the best-fit parameters, and we calculate $\Delta\chi^2$ values relative to this point. A color scale bar along the right side of the contour shows levels of $\Delta\chi^2$ values. The significances of the existence of linear polarization are 3.7σ for GRB 110301A and 3.3σ for GRB110721A, respectively.